Identifying Influential Nodes in a Network Model of Epilepsy

Article *in* Journal of Nonlinear Science · April 2019

DOI: 10.1007/s00332-019-09545-4

CITATIONS
0

READS
43

4 authors, including:

Amber Afelin
Carnegie Mellon University
1 PUBLICATION **0** CITATIONS
SEE PROFILE

Christian G Fink
Gonzaga University
18 PUBLICATIONS **86** CITATIONS
SEE PROFILE

Journal of Nonlinear Science
https://doi.org/10.1007/s00332-019-09545-4

Journal of Nonlinear Science

Identifying Influential Nodes in a Network Model of Epilepsy

Joseph Emerson[1] · **Amber Afelin**[2] · **Viesulas Sliupas**[3] · **Christian G. Fink**[4]

Received: 8 September 2018 / Accepted: 3 April 2019

Abstract
A significant proportion of individuals with epilepsy suffer from intractable forms of the disease. Current evidence suggests that pathological brain connectivity could be a major contributor to the propagation of focal seizures, constituting a possible cause for some forms of intractable epilepsy. Currently, however, the precise network structures that underpin epileptic brain connectivity are poorly understood. In this study, we use a computational model to simulate focal seizure spread in the macaque cortical connectome. We then use the results to propose a novel network centrality measure (called "Ictogenic Centrality") that accurately identifies which nodes are most effective in propagating seizures. In the framework presented, ictogenic centrality outperforms other standard centrality measures in correctly identifying ictogenic nodes, exhibiting high accuracy (0.947), specificity (0.939), and sensitivity (0.964). Ictogenic centrality is degree based and relies on only a single free parameter, making it useful and efficient to compute for large networks. Our results suggest that baseline brain connectivity may predispose the temporal and frontal lobes toward ictogenicity even in the absence of any overtly pathological network reorganization.

Keywords Epilepsy · Seizure · Connectome · Centrality

Mathematics Subject Classification 92B20 · 92B25 · 05C82

1 Introduction

Epilepsy is the fourth-most prevalent neurological disorder (behind cerebrovascular disease, dementia, and migraine disorders), affecting at least 0.5% of all people worldwide (World Health Organization 2006). While approximately two-thirds of this population can be effectively treated through medication (Kwan and Sander 2004), and another 8–10% through surgical intervention, the remainder fall to attain full

Communicated by Paul Newton.

Extended author information available on the last page of the article

Published online: 13 April 2019

seizure control (Mormann et al. 2006), reflecting our inadequate understanding of the manifold mechanisms underpinning seizure generation.

One possibility is that some forms of intractable epilepsy are the result of pathological brain connectivity (Spencer 2002; Bartolomei et al. 2017). Thalamocortical connections (Crunelli and Leresche 2002; Kim et al. 2014) and interhemispheric connections (Ji et al. 2014) may be compromised in instances of generalized epilepsy, in which seizures arise in both hemispheres simultaneously. Focal epilepsies, on the other hand, are a diverse group of conditions in which seizures originate in localized region(s) of the brain before potentially spreading. Focal epilepsies can be notoriously resistant to anti-epileptic drugs (Semah et al. 1998; Engel et al. 2003; Sørensen and Kokaia 2013). In the past few decades, both basic and clinical studies have increasingly supported an understanding of focal epilepsy as a network phenomenon (Wendling et al. 2010; Bartolomei et al. 2017; Shah et al. 2018). At the local circuit scale, it has been shown that recurrent connections between granule cells in the dentate gyrus are a hallmark of certain forms of focal epilepsy associated with the temporal lobe (referred to as temporal lobe epilepsy, or TLE) (Buckmaster et al. 2002; Morgan and Soltesz 2008). On a larger scale, a recent diffusion MRI study of patients with TLE identified particular connections from the temporal lobe whose strength predicted the success or failure of surgical treatment with high accuracy (Bonilha et al. 2015). More generally, several clinical studies indicate that both structural and functional brain networks in patients with focal epilepsy tend to exhibit higher average path lengths and clustering coefficients than in healthy controls (van Diessen et al. 2014; Bernhardt et al. 2015; Bonilha et al. 2012; Vaessen et al. 2014; Liao et al. 2010). Other studies suggest that brain lesions in patients with TLE tend to be concentrated in "hub" nodes (as identified in diffusion MRI-derived brain networks) (Crossley et al. 2014).

While the foregoing findings provide strong evidence of aberrant connectivity associated with some forms of focal epilepsy, we currently understand very little about how particular connectivity patterns facilitate seizure spread. Given current clinical and experimental limitations in recording brain activity, computational modeling may offer a way forward. Many approaches have been proposed for modeling large-scale seizure dynamics (Lytton 2008; Wendling et al. 2002; Da Silva et al. 2003; Breakspear et al. 2005; Taylor and Baier 2011), and several are amenable to network models. Taylor et al. formulated a network model to investigate the emergence of spike-and-wave discharges observed in the EEG of patients with *generalized* epilepsy (Taylor et al. 2013), and Benjamin et. al. also investigated generalized epilepsy (Benjamin et al. 2012) by refining an earlier network model (Kalitzin et al. 2010). Goodfellow et al. (2016) and Sinha et al. (2016) devised network models of focal epilepsy that showed promise in identifying seizure foci in patients with epilepsy. These studies did not, however, attempt to elucidate general connectivity patterns that facilitate seizure spread.

Recently, Jirsa et al. (2014) introduced a phenomenological model of seizure dynamics (dubbed "Epileptor") that reproduced the bifurcation structure observed in transitions into and out of seizing states for several different species. This model was used to simulate seizure spread in individual patients with focal epilepsy (Proix et al. 2017), and the results were compared with patients' clinical records of seizure propagation. Simulations more accurately predicted seizure propagation when using

patients' individual, diffusion MRI-derived connectomes than when using randomly rewired versions of their connectomes, underscoring the importance of large-scale connectivity to understand seizure dynamics. Similar to the previous studies, however, this work did not attempt to identify general patterns of connectivity that correlate with seizure severity.

The few other studies that have attempted to do so have found only limited success (Terry et al. 2012; Hutchings et al. 2015). Hutchings et al. (2015) developed a computational model in which seizures tended to start in the temporal lobe, matching clinical data. They ran their model on individual patient connectomes defined through diffusion tensor imaging, and they identified the top ten spreading nodes for both patients with epilepsy and healthy controls. They found that five nodes were common to both groups, and that these nodes showed high degree and low clustering, suggesting they could be considered hubs. This study did not, however, attempt to develop a network measure to distinguish ictogenic from non-ictogenic nodes. Terry et al. (2012) developed a computational model of epilepsy in a toy four-node network that could generate either focal, secondary generalized, or primary generalized seizures, depending on the network structure. They showed that decreasing overall network connectivity could increase the frequency of seizure events. Again, however, they did not attempt to develop a network measure to identify ictogenic versus non-ictogenic nodes and/or networks.

This study uses the Epileptor model of focal epilepsy to propose a novel centrality measure for identifying connectivity patterns that facilitate seizure spread. Unlike previous network-based epilepsy models, we investigate seizure propagation in the macaque connectome (Bakker et al. 2012). Most whole-brain simulations of epileptic seizures have used diffusion MRI structural data or correlation-based functional data to define brain connectivity (Petkov et al. 2014; Hutchings et al. 2015), both of which omit directionality of connections. This is particularly problematic in modeling seizure propagation, since a brain region with predominantly outgoing connections should presumably spread seizures much more effectively than a region with predominantly incoming connections.

Based on simulation results using the directed macaque connectome, we propose a highly accurate centrality measure for predicting the extent of seizure spread from a particular epileptic focus. Results also suggest that baseline brain connectivity predisposes particular brain regions (such as the temporal and frontal lobes) to focal epilepsy, even in the absence of pathological network reorganization.

2 Methods

2.1 Epileptor Model

The equations governing the dynamics of brain region i in the Epileptor model are (Proix et al. 2017; Jirsa et al. 2017):

$$\dot{x}_{1,i} = y_{1,i} - f_1(x_{1,i}, x_{2,i}) - z_i + I_1 \tag{2.1}$$

$$\dot{y}_{1,i} = 1 - 5x_{1,i}^2 - y_{1,i} \tag{2.2}$$

$$\dot{z}_i = \frac{1}{\tau_0}\left(4(x_{1,i} - x_{0,i}) - z_i - \sum_{j=1}^{N} K_{ij}(x_{1,j} - x_{1,i})\right) \tag{2.3}$$

$$\dot{x}_{2,i} = -y_{2,i} + x_{2,i} - x_{2,i}^3 + I_2 + 0.002g(x_{1,i}) - 0.3(z_i - 3.5) \tag{2.4}$$

$$\dot{y}_{2,i} = \frac{1}{\tau_1}\left(-y_{2,i} + f_2(x_{2,i})\right) \tag{2.5}$$

where

$$f_1(x_{1,i}, x_{2,i}) = \begin{cases} x_{1,i}^3 - 3x_{1,i}^2 & \text{if } x_{1,i} < 0 \\ \left(x_{2,i} - 0.6(z_i - 4)^2\right) x_{1,i} & \text{if } x_{1,i} \geqslant 0 \end{cases} \tag{2.6}$$

$$f_2(x_{2,i}) = \begin{cases} 0 & \text{if } x_{2,i} < -0.25 \\ 6(x_{2,i} + 0.25) & \text{if } x_{2,i} \geqslant -0.25 \end{cases} \tag{2.7}$$

$$g(x_{1,i}) = \int_{t_0}^{t} e^{-\gamma(t-\tau)} x_{1,i}(\tau)\mathrm{d}\tau \tag{2.8}$$

Equations (2.1)–(2.3) constitute the heart of the model, representing a Hindmarsh–Rose square wave burster (Hindmarsh and Rose 1984; Hindmarsh and Cornelius 2005) with the same bifurcation structure (saddle-node onset and homoclinic offset) as observed in human focal seizures (Jirsa et al. 2014). Equations (2.4)–(2.5) generate spike-and-wave events as observed clinically, and $x_1 + x_2$ models the simulated LFP. The coupling of brain regions through the variable x_1 represents disruption of extracellular ion concentration induced by high levels of neural activity (Proix et al. 2014). We used the parameters originally employed by Jirsa et al. (2014): $\tau_0 = 2857$, $\tau_1 = 10$, $I_1 = 3.1$, $I_2 = 0.45$, and $\gamma = 0.1$, with 256 time steps corresponding to 1 s of real time (Proix et al. 2014).

The variable x_0 is a bifurcation parameter that separates epileptic dynamics ($x_0 > -2.05$) from non-epileptic dynamics ($x_0 < -2.05$) in a single node. In our simulations, we set $x_0 = -2.12$ for all nodes except one, the simulated epileptic focus, for which we set $x_0 = -1.60$. (Note that we also ran simulations for other non-epileptic x_0 values—see Fig. 12.) This resulted in the epileptic focus undergoing periodic seizures, which spread throughout the network to varying degrees depending on the connectivity of the focus. The coupling matrix, K, was defined according to the macaque cortical connectome, and all nonzero entries, K_{ij}, were set to 0.20, which was the minimum value for which seizures spread appreciably for any node. All simulations were conducted using Heun numerical integration with a time step of 0.04. Finally, following (Proix et al. 2017), uncorrelated Gaussian noise with zero mean and a variance of 0.0025 was added to x_2 and y_2 for all nodes.

2.2 Quantifying Seizure Spread

For each seizure undergone by an epileptic focus, the ensuing network *seizure event* was defined to last until no nodes continued to seize. As illustrated in Fig. 1a, some

seizure events spread throughout the entire network, while others did not spread at all. For each epileptic focus, a simulation lasting 585 seconds was run, resulting in approximately 140 seizure events. The average number of nodes enlisted across all seizure events was then calculated for each node. Note that for influential nodes, this average typically included seizure events that encompassed the entire network as well as events that did not spread at all.

2.3 Macaque Connectome

The CoCoMac database (Kötter 2004; Bakker et al. 2012) aggregates the results of hundreds of macaque tract-tracing studies, which involve injecting tracer molecules into a neural population and using light microscopy to track their axonal transport. By controlling whether tracer molecules are injected into neural soma and subsequently transported to synapses or vice versa, the direction of neural connections may be established. The CoCoMac database is then used to construct entire cortical connectomes. Here, we use the CoCoMac-derived, single-hemisphere connectome developed by Kaiser and Hilgetag (2006), which features directed, unweighted connections between 94 macaque cortical regions.

2.4 Comparison Centrality Measures

We compared the performance of our ictogenic centrality measure (discussed in detail in the Sect. 3) to several other centrality measures: out-degree (number of outgoing connections for a given node), in-degree (number of incoming connections for a given node), outgoing PageRank, standard (incoming) PageRank, control centrality, and Latent Ictogenic Centrality.

2.4.1 Standard and Outgoing PageRank

The standard PageRank algorithm rewards nodes for the *incoming* connections they receive, weighting each connection by the inverse of the out-degree of the sending node (Page et al. 1999). (This scheme was originally motivated by the intuition that the more hyperlinks a website receives, the higher its score should be, with links coming from websites that send out relatively few hyperlinks weighted more, since those websites are presumably more discriminating.) The PageRank score for the ith node in a network with adjacency matrix A_{ij} (with connections running from j to i) is calculated by iterating the following formula until convergence is reached:

$$x_i = \alpha \sum_{j=1}^{N} \frac{A_{ij}}{k_j^{\text{out}}} x_j + (1 - \alpha) \tag{2.9}$$

In quantifying the influence of a node in spreading epileptic seizures, we hypothesized its score should be based on the number of connections it *sends out*, with connections weighted more if the receiving node has a smaller in-degree (since incoming con-

nections from healthy nodes help prevent the seizure from spreading). We therefore employed a modified PageRank algorithm, using the power method to solve the following equation:

$$x_i = \alpha \sum_{j=1}^{N} \frac{A_{ji}}{k_j^{\text{in}}} x_j + (1 - \alpha) \tag{2.10}$$

In both cases, we set α to the standard value of 0.85.

2.4.2 Control Centrality

This centrality measure was recently introduced specifically for characterizing epileptic brain networks (Khambhati et al. 2016). It is based on the theoretical result that dynamical networks with linear coupling are more synchronizable when exhibiting smaller spread in the eigenvalues of the Laplacian matrix (Pecora and Carroll 1998), defined as $L_{ij} = \delta_{ij} \sum_k A_{ik} - A_{ij}$. The propensity for synchronization of an undirected network may therefore be characterized by the ratio $\lambda_{\max}/\lambda_2$, where $\lambda_{\max}$ is the largest eigenvalue of L and λ_2 the smallest. (λ_1 is always trivially zero since L's rows sum to zero.) Smaller values of $\lambda_{\max}/\lambda_2$ reflect smaller spread in the eigenvalue spectrum, and therefore imply greater propensity for network synchronization. The analogous measure $\lambda^r_{\max}/\lambda^r_{\min}$, where $\lambda^r_{\min}$ is the smallest nonzero real eigenvalue component, may be used for directed networks, whose eigenvalues are in general complex (Hwang et al. 2005).

If we define $s \equiv \lambda^r_{\max}/\lambda^r_{\min}$, then we can quantify node i's contribution to network synchronization according to

$$c_i = \frac{s_{N\setminus i} - s_N}{s_N}, \tag{2.11}$$

where s_N is the eigenvalue spread for the full network, and $s_{N\setminus i}$ is the eigenvalue spread with node i and all of its connections removed. Positive/negative values for c_i correspond to the presence of node i increasing/decreasing the network's propensity for synchronization.

2.5 Network Formation Models

Epileptor dynamics were used to simulate seizure spread on networks constructed using two different network formation models. The Price model (de Solla Price 1976) generated a scale-free network, and the Watts–Strogatz model (Watts and Strogatz 1998) generated a random network. In both models, every node had a the same out-degree.

2.5.1 Price Model

The Price model is a lesser-known predecessor of the Barabàsi–Albert model (Barabási and Albert 1999) for generating networks with power-law degree distributions. The primary difference is the Price model is directed, and was originally formulated to model citation networks. We used the Price model to generate a 250-node network with

power-law in-degree distribution and uniform out-degree ($k_{\text{out}} = 50$ for all nodes). In our implementation, we started with 51 nodes, each of which sent connections to the other 50. Nodes were then added to the network one at a time, with each new node sending 50 outgoing connections. The probability of an existing node receiving a new connection was directly proportional to its in-degree, so that nodes "born" early in the process tended to have higher final in-degree than those born later. It can be shown that this process results in an in-degree distribution with an exponent of ≈ 2 (Newman 2018).

2.5.2 Watts–Strogatz Model

In order to generate a random network which controlled for out-degree, we employed the Watts–Strogatz model with a rewiring probability of 1. Our network had 100 nodes, initially arranged in a ring such that each node sent connections to the ten nearest neighbors on either side (so that $k_{\text{out}} = 20$ for all nodes). With a rewiring probability of 1, *every* connection was rewired to a new, randomly selected destination node (while keeping the source node the same, thus preserving uniform out-degree).

3 Results

3.1 Simulation Results

In seeking to formulate a centrality measure to identify which nodes are most effective in spreading seizures, we first ran simulations to establish "ground truth" results. These results were then used to quantify the accuracy of various centrality measures in identifying influential nodes. Simulations were conducted by placing Epileptor dynamics at each node of the macroscale macaque connectome (Kaiser and Hilgetag 2006), modeling the local field potential recorded from each of 94 brain regions. The macaque connectome was used because its connections are directed (in contrast with the undirected connections in MRI-derived human connectomes), and information concerning directionality is important to accurately quantify many graph-theoretic measures in brain networks (Kale et al. 2018). The adjacency matrix of the macaque connectome used in this study is visualized in Fig. 1c.

In each simulation, one node—the "ictogenic node"—was induced to perpetually undergo seizures (modeling the seizure focus), and the remaining 93 were set to an intrinsically non-seizing regime. (See Sect. 2 for more details.) These otherwise healthy nodes would not seize in isolation, but were capable of suffering seizures in our simulations due to coupling with the ictogenic node. The ictogenic node's influence was then defined to be the average number of healthy nodes enlisted in each seizure event.

Figure 1b shows voltage traces for two example ictogenic nodes: the middle temporal area (MT) and the lateral ventral intraparietal area (VIPl). Figure 1a depicts network-wide seizure spread for these same ictogenic nodes. Node MT is particularly interesting, since when it is ictogenic the seizure does not spread at all, even though MT has the largest out-degree of any node in the entire network. This point will be further

explored shortly. Figure 1d summarizes the simulated spreading ability of each node. These results accord with clinical data indicating that epileptic foci are identified most frequently in the temporal lobe, followed by the frontal lobe, then the parietal lobe, and least frequently in the occipital lobe (Prayson and Estes 1995; Elsharkawy et al. 2008; Cossu et al. 2005; Sveinbjornsdottir and Duncan 1993; Maynard et al. 2017; Manford et al. 1992). The 28 nodes which effectively spread the seizure throughout the network (highlighted in Fig. 1d) were classified as "influential seizers." It was these nodes we wished to accurately identify using a connectivity-based centrality measure.

3.2 Centrality Measure

The first step in formulating such a centrality measure was determining why out-degree alone was a poor predictor of epileptic influence. As mentioned above, the node with the single largest out-degree (brain region MT) was incapable of spreading its seizure to even one other node. Since previous studies of the Epileptor model have shown that connections from healthy nodes can prevent seizures from occurring in ictogenic nodes (Proix et al. 2014), we investigated whether an ictogenic node's in-degree played a role in its epileptic influence. Figure 2 shows the results of simulations in which incoming connections to MT were progressively deleted. With its full set of 38 incoming connections, MT was incapable of spreading a seizure to any other nodes. As more incoming connections were severed, however, it enlisted more and more nodes in its seizure events. Note, however, that Fig. 2c shows that node MT suffered seizures even when the rest of the network did not. The healthy nodes were not abolishing the ictogenic node's seizures, as previous studies have can theoretically occur when coupling is very strong (Proix et al. 2014). Instead, Fig. 2a suggests the incoming connections shortened the ictogenic node's seizures to the point that they could not spread to any neighbors. This phenomenon was ubiquitous among non-influential, high out-degree nodes. See Sect. 5.1 for three other examples.

Further investigation showed that incoming connections could help suppress seizure spread not only by terminating on the ictogenic node itself, but also by terminating on its immediate neighbors. (Here and henceforth we define "neighbors of the ictogenic node" to be nodes that *receive connections from*, but do not necessarily send connections to, the ictogenic node.) Intuitively, connections coming into the ictogenic node exert a protective influence by pulling the ictogenic node closer to the non-seizing regime (via Eq. 2.3), whereas connections coming into *neighbors* of the ictogenic node help prevent initial spread of the seizure. The dynamics of the system are such that incoming connections to the ictogenic node have roughly equal protective effect regardless of where they originate. Incoming connections to ictogenic neighbors, however, are more effective in suppressing seizure spread when they originate from *non-neighboring* nodes, since neighboring nodes' dynamics are somewhat compromised by ictogenic input (see Sect. 5.2 in the Supplementary Material for further analysis of this effect).

Based on these observations, we formulated a measure called Latent Ictogenic Centrality (LIC) that quantifies an ictogenic node's ability to spread seizures, so long as the node's in-degree is not too large. The LIC of node i is defined as

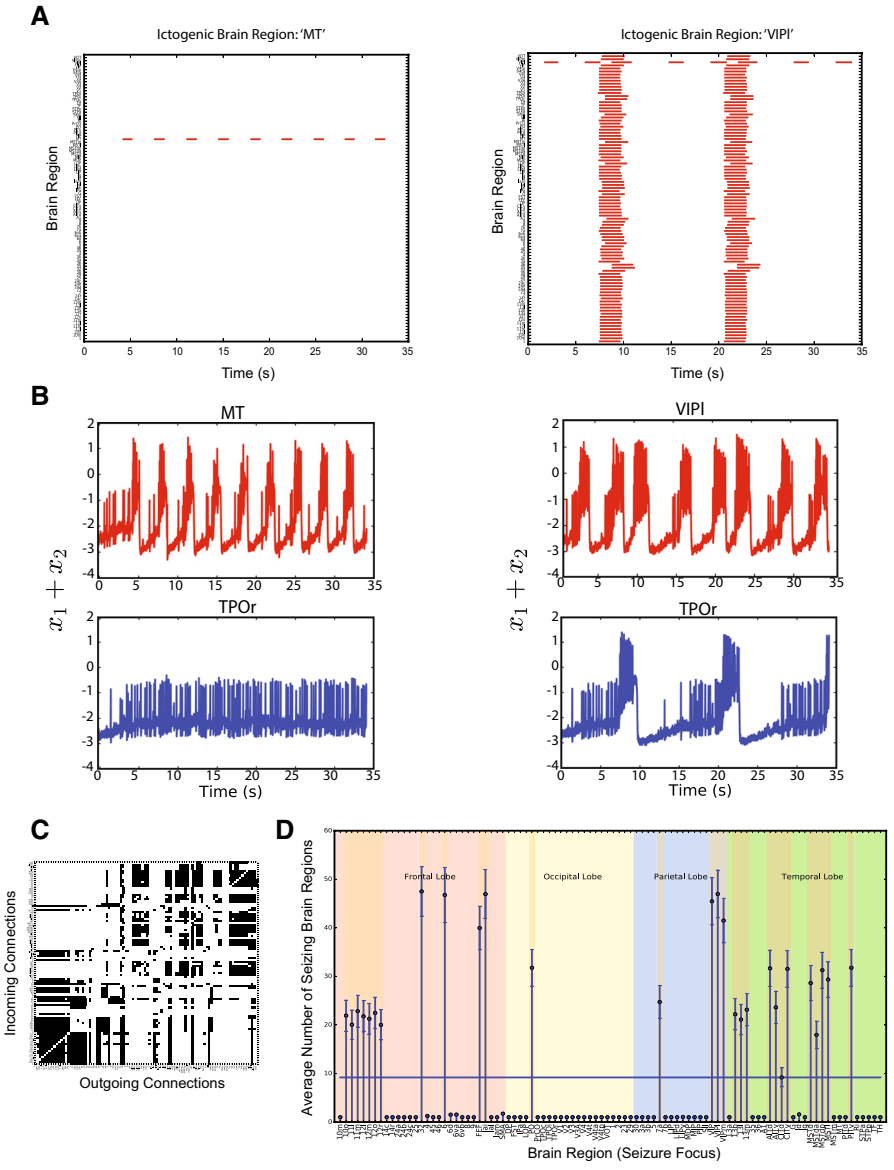

Fig. 1 Influential nodes in a computational model of seizure propagation. **a** Example raster plots depicting seizure incidence and duration throughout the network for ictogenic nodes MT (left pane) and VIPl (right pane). The seizure fails to spread at all in the first case, and it spreads to the entire network in the second case. **b** Example voltage traces obtained using the Epileptor model of seizure dynamics. Red traces represent voltage of the ictogenic nodes MT (middle temporal area, left pane) andVIPl (lateral ventral intraparietal area, right pane). Blue traces represent voltage of brain region TPOr (rostral temporo-parieto-occipital area), which receives connections from both MTandVIPl. Note howTPOr does not seize whenMTis ictogenic, and it does seize when VIPl is ictogenic. **c** Binary, directed adjacency matrix for the macaque cortical connectome used in these simulations. **d** Average number of nodes each seizure spreads to when starting at each ictogenic node as the seizure focus. The network naturally segregates into influential and non-influential nodes (above and below the horizontal line, with influential nodes highlighted) (Color figure online)

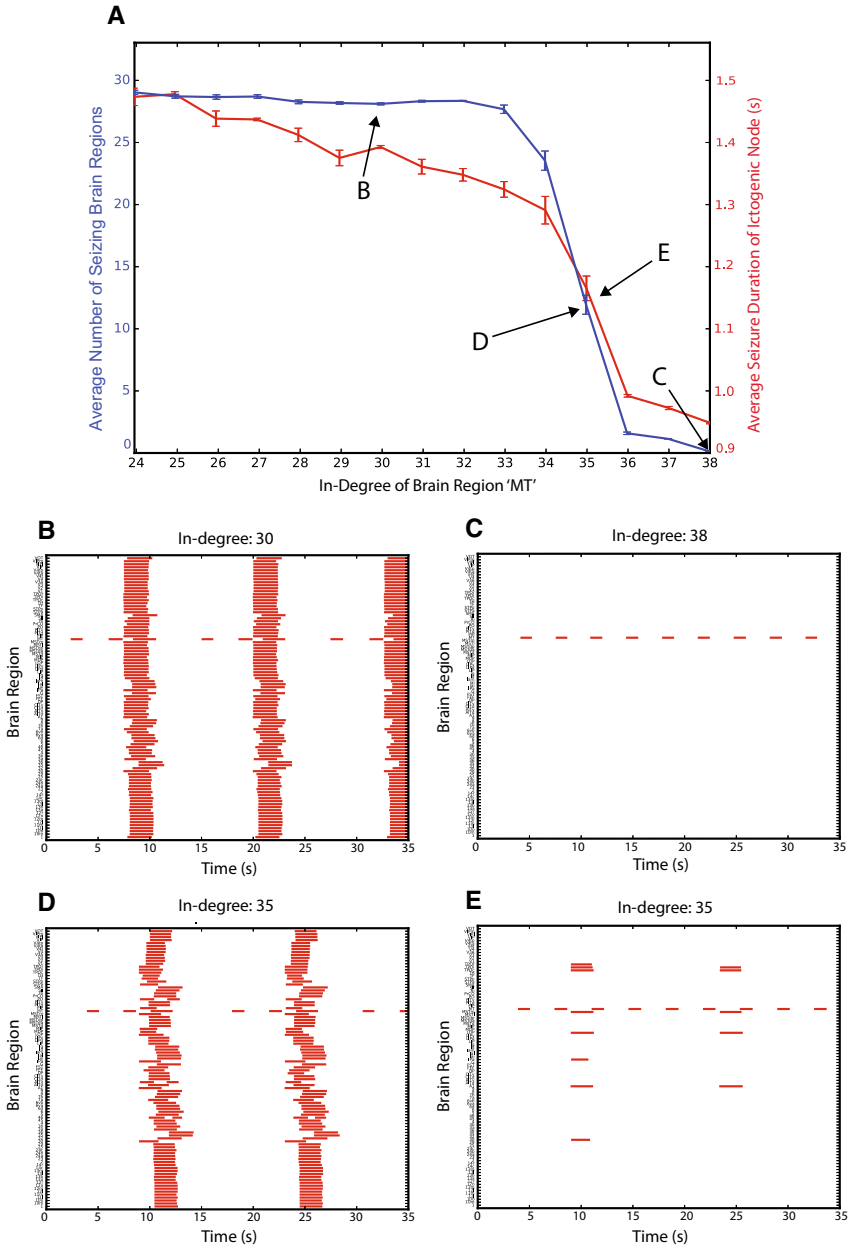

Fig. 2 Effect of in-degree on ictogenic node's spreading ability. **a** Average number of nodes enlisted per seizure (blue line) and average seizure duration of node MT (red line) as a function of the in-degree of ictogenic node MT. Fifty simulations were conducted for each value of MT's in-degree (whose standard value was 38), with a different set of randomly selected incoming connections deleted in each simulation. Error bars reflect the standard error of the mean over the fifty trials. **b–e** Raster plots depicting increasing seizure spread as more incoming connections to MT were deleted. **d**, **e** Illustrate how in the transition region, quite different network dynamics resulted from different sets of incoming connections being randomly deleted (Color figure online)

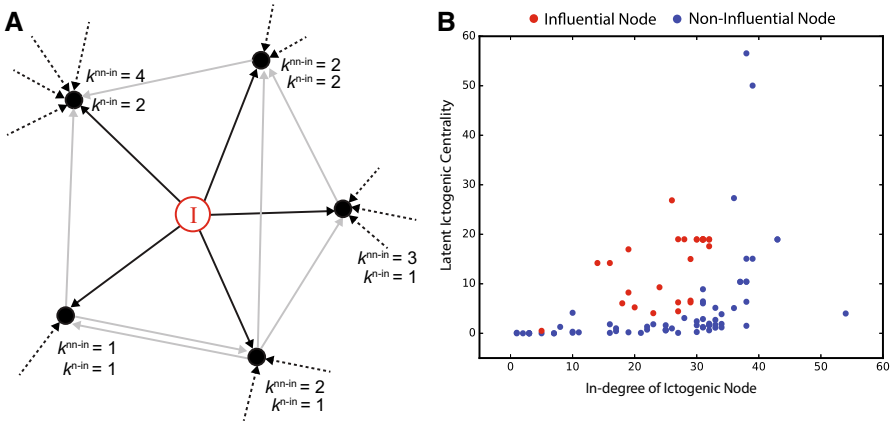

Fig. 3 Using Latent Ictogenic Centrality (LIC) to identify influential seizers. **a** Example network illustrating the concept of non-neighboring in-degree. Connections from the ictogenic node (labeled "I") to its neighbors are shown in solid black, while connections between ictogenic neighbors are colored gray. Connections coming into ictogenic neighbors from non-neighbors are depicted as dashed lines. These are the connections that determine the non-neighboring in-degree ($k^{\mathrm{nn-in}}$) of each ictogenic neighbor. **b** Scatter plot showing the LIC and in-degree of each node in the macaque connectome. Influential seizers (as identified from simulation results) are colored red and non-influential nodes are colored blue, illustrating how these two classes are quite distinct with respect to these measures. Note that in some cases several points lie exactly on top of one another (Color figure online)

$$\mathrm{LIC}(i) = \sum_{j \in \Gamma_i} \frac{1}{k_j^{\mathrm{nn-in}(i)} + a\, k_j^{\mathrm{n-in}(i)} + \frac{1}{2}}. \tag{3.1}$$

Here, Γ_i is the set of all nodes that receive connections from node i, $k_j^{\mathrm{nn-in}(i)}$ is the non-neighboring in-degree of node j with respect to node i, equal to $\sum_{k \neq i} A_{jk}(1 - A_{ki})$, and $k_j^{\mathrm{n-in}(i)}$ is the neighboring in-degree of node j with respect to node i, equal to $\sum_{k \neq i} A_{jk} A_{ki}$. (Figure 3a gives a toy example of calculating non-neighboring in-degree and neighboring in-degree values.) a is a parameter between 0 and 1 that reflects the diminished protective effect of incoming connections from neighbors, compared to non-neighbors, while the factor of $\frac{1}{2}$ simply prevents division by 0. Intuitively, the denominator quantifies the protective effect of incoming connections to node j. The smaller the denominator, the more likely node j is to be enlisted in a seizure originating from node i, which results in a relatively large contribution to node i's LIC.

For the macaque connectome, we found that non-neighboring connections exerted so much greater protective influence than neighboring connections that we could eliminate the $k_j^{\mathrm{n-in}(i)}$ term (see Sect. 5.3 in the Supplementary Material), simplifying Eq. 3.1 to

$$\mathrm{LIC}(i) = \sum_{j \in \Gamma_i} \frac{1}{k_j^{\mathrm{nn-in}(i)} + \frac{1}{2}}. \tag{3.2}$$

The scatter plot in Fig. 3b suggests that combining LIC with ictogenic in-degree (as discussed in Fig. 2) does a remarkably good job separating "influential seizers"

from non-influential nodes. We therefore combined them into a novel measure, which we call Ictogenic Centrality (IC):

$$\mathrm{IC}(i) = \left(\sum_{j \in \Gamma_i} \frac{1}{k_j^{\mathrm{nn-in}(i)} + \frac{1}{2}} \right) \; H\left(-(k_i^{\mathrm{in}} - k_{\mathrm{thresh}}^{\mathrm{in}}) \right) \tag{3.3}$$

Here, $H(\cdot)$ is the Heaviside function, and $k_{\mathrm{thresh}}^{\mathrm{in}}$ is the in-degree above which a node's IC is set to zero, regardless of its LIC.

3.3 Performance of IC

In Fig. 4, we compare the performance of Ictogenic Centrality (with $k_{\mathrm{thresh}}^{\mathrm{in}} = 32$, as suggested by Fig. 3b) with several other centrality measures commonly used to analyze spreading processes and epileptic influence. In addition to out-degree, we explored a modified version of PageRank that rewards nodes for their outgoing connections. We also compared to control centrality, a measure that uses the graph Laplacian to characterize the propensity for synchronization of a network, and which has recently been applied to analysis of epileptic brain networks (Khambhati et al. 2016) (see Sect. 2 for more details). Finally, we included comparisons with in-degree, standard PageRank, and Latent Ictogenic Centrality as well. ROC curves were constructed for each measure by classifying nodes as influential/non-influential if they scored above/below some threshold, and calculating the sensitivity (true positive rate) and specificity (true negative rate) as the threshold was varied.

Ictogenic Centrality clearly shows a much larger area under the ROC curve than all other comparison measures. (The poor performance of control centrality may be due to its assumption that seizures are hypersynchronous events, whereas in the network Epileptor model seizures more closely resemble a spreading phenomenon. Control centrality is therefore expected to perform better in models of generalized epilepsy.) Figure 5 compares performance results for four measures using the optimal threshold for each measure, highlighting true positives, false positives, and false negatives, while Table 1 delineates the accuracy, sensitivity, and specificity for each centrality measure. These results suggest that Ictogenic Centrality far outperforms other connectivity-based centrality measures in identifying which nodes will most effectively spread seizures in the Epileptor model. This conclusion holds over various values of the most important Epileptor parameter, x_0 (see Sect. 5.4).

3.4 IC-Directed Intervention

Ictogenic Centrality could also be used to efficiently remove outgoing connections from ictogenic nodes in order to eliminate seizure spread in the Epileptor model. We conducted simulations in which, for each influential node, outgoing connections were removed one at a time, in ascending order of non-neighboring in-degree of the connections' terminal nodes. These connections were progressively removed until

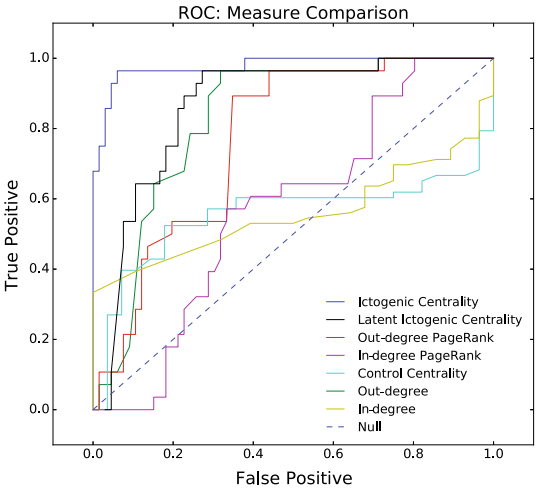

Fig. 4 ROC performance comparison of Ictogenic Centrality with other centrality measures. Each measure was thresholded in order to identify influential seizers. Each measure's classification was then compared with the "known" set of influential seizers (from simulation results) in order to calculate true positive and false positive rates as the threshold was varied. The area under the curve is much larger for Ictogenic Centrality than for any of the other measures

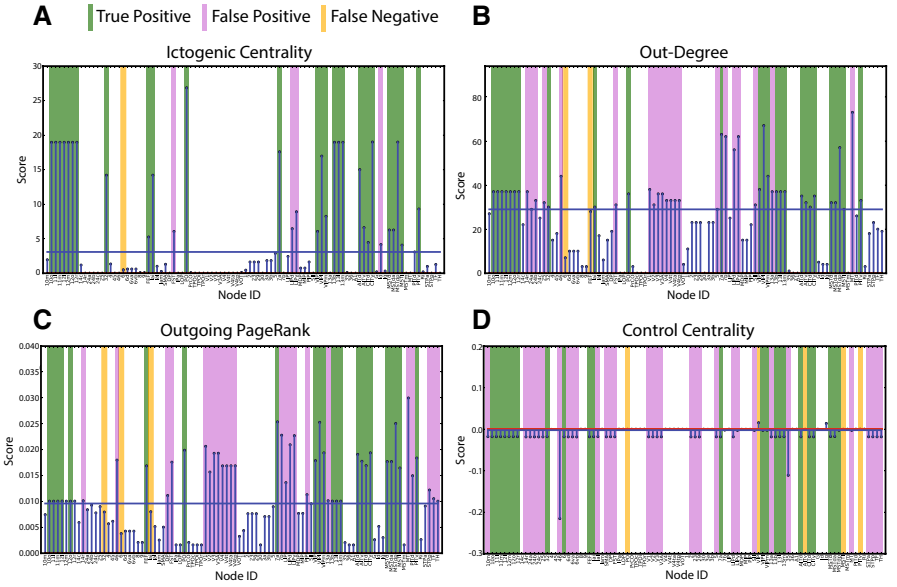

Fig. 5 Comparison of measure performance using optimal thresholds. Panels show the score of each node according to the corresponding centrality measure (**a** Ictogenic Centrality, **b** Out-Degree, **c** Outgoing PageRank, **d** Control Centrality). Green highlights are true positives, purple highlights are false positives, and yellow highlights are false negatives. The horizontal bar represents the optimal threshold, defined as the value which yielded the shortest distance from the $(0, 1)$ coordinate on the ROC curve (Color figure online)

seizure spread was completely repressed. We also ran simulations employing random, rather than IC-guided, removal of connections, and compared which approach tended to require fewer deletions for seizure freedom. Figure 6 shows the number of connections removed for each influential node, following each approach. IC-directed

Table 1 Performance metrics for measure comparison.

	Ictogenic Centrality	Latent Ictogenic Centrality	Outgoing PageRank	Incoming PageRank	Control Centrality	Out-degree	In-degree
Accuracy	0.947	0.809	0.723	0.447	0.606	0.755	0.543
Specificity	0.939	0.773	0.652	0.364	0.515	0.682	0.394
Sensitivity	0.964	0.893	0.893	0.643	0.821	0.929	0.893
Area under curve	0.977	0.863	0.769	0.573	0.576	0.828	0.558

Accuracy, specificity, and sensitivity are shown for each centrality measure. Area under the curve is taken from receiver operating characteristic (ROC) curve

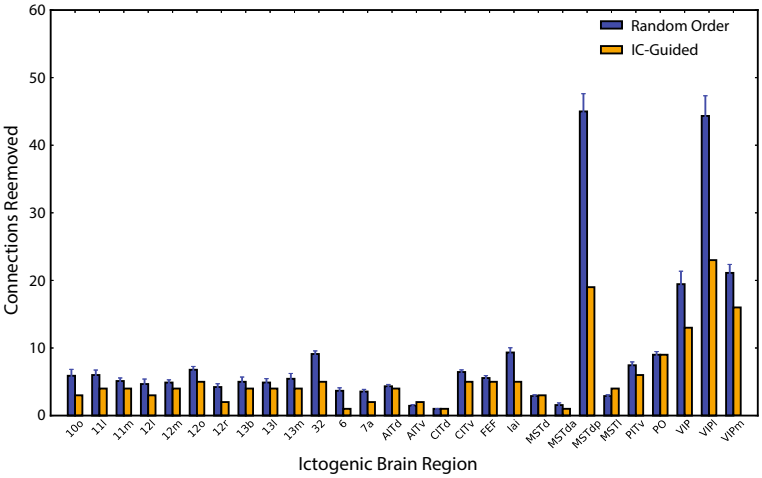

Fig. 6 Random versus IC-guided removal of outgoing connections to eliminate seizure spread. For each influential node, outgoing connections were progressively removed according to the non-neighboring in-degree of the connection's terminus. The total number of connections removed in order to first eliminate seizure spread was measured. These values (yellow bars) are compared with the average number of connections which were *randomly* removed in order to eliminate seizure spread. Blue bars represent average values over nine simulations, and error bars indicate standard error of the mean (Color figure online)

deletion permitted the removal of the same or fewer connections than random deletion (on average) for all but two influential nodes.

3.5 IC in Scale-Free and Random Networks

Finally, in order to investigate the generality of IC, we conducted simulations of Epileptor seizure spread on both random and scale-free (SF) network architectures. We then compared IC's performance with the same centrality measures as in the macaque connectome. Both networks featured the same out-degree for every single node, thereby controlling for the most obvious mode of ictogenic influence. This was accomplished by using the Watts–Strogatz model (Watts and Strogatz 1998) to

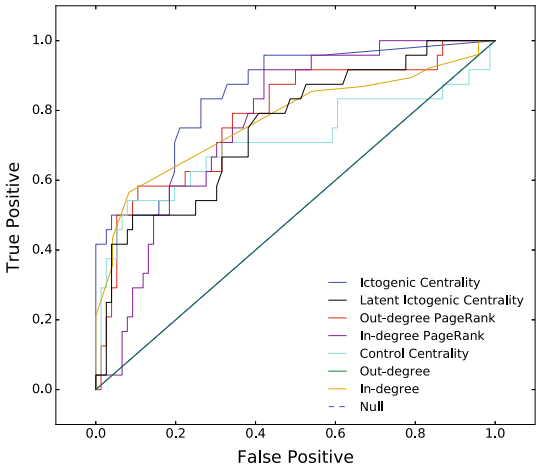

Fig. 7 Performance of IC in a random network. Various centrality measures were thresholded in order to identify putative influential seizers within a random network (generated using the Watts–Strogatz model with a rewiring probability of 1). ROC curves were generated by sweeping through all possible thresholds and quantifying true and false positive rates. Optimal IC performance was obtained using $k^{\text{in}}_{\text{thresh}} = 21$. IC outperformed all other centrality measures (see Table 2). Out-degree follows the null line because all nodes in the network had the same out-degree (20)

generate the random network and the Price model (de Solla Price 1976) for the SF network (see Sect. 2 for more details). The random network was composed of 100 nodes, each with an out-degree of 20, and the SF network was composed of 250 nodes, each with an out-degree of 50. Coupling strengths were set to the lowest values that resulted in appreciable seizure spread throughout the network.

Figures 7 and 8 depict ROC curve performance comparisons for the random and SF networks, respectively. IC outperformed all centrality measures in the random network, and in the SF network it outperformed all measures except for LIC and outgoing PageRank (which all essentially tied). Performance values are quantified in Tables 2 and 3. Overall, these results suggest that IC is a robust measure for identifying influential seizers in generic networks with Epileptor dynamics.

4 Discussion

In this study, we used the Epileptor dynamical equations to formulate a network-based model of focal epilepsy on the macaque cortical connectome. The macaque connectome was used because it is directed, and it has been shown to be similar to the human connectome at macroscopic scales (Goulas et al. 2014). In addition, previous studies have used the macaque connectome to explore the relationship between structural and functional connectivity in the human brain (Kötter and Wanke 2005; Ghosh et al. 2008; Deco et al. 2009).

Network Epileptor simulations produced realistic results, with brain regions in the temporal and frontal lobes being most effective in spreading focal seizures (Fig. 1d),

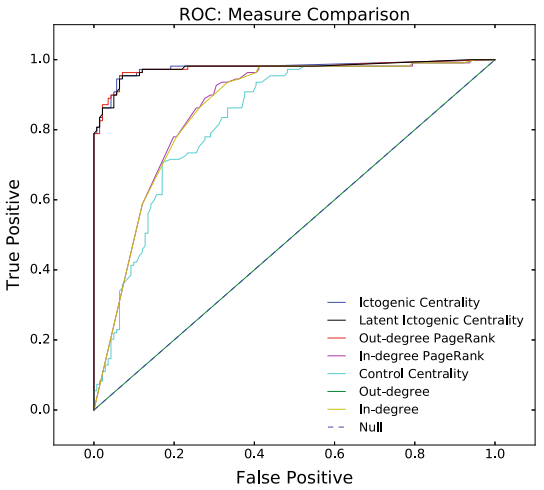

Fig. 8 Performance of IC in a scale-free network. Various centrality measures were thresholded in order to identify putative influential seizers within a scale-free network (generated using the Price model). ROC curves were generated by sweeping through all possible thresholds and quantifying true and false positive rates. Optimal IC performance was obtained using $k^{\text{in}}_{\text{thresh}} = 7$. IC outperformed all measures except LIC and outgoing PageRank, which it essentially tied (see Table 3). Out-degree follows the null line because all nodes in the network had the same out-degree (50)

Table 2 Performance metrics in a random network

	Ictogenic Centrality	Latent Ictogenic Centrality	Outgoing PageRank	Incoming PageRank	Control Centrality	Out-degree	In-degree
Accuracy	0.760	0.650	0.690	0.700	0.690	0.240	0.650
Specificity	0.736	0.618	0.658	0.697	0.684	0.000	0.565
Sensitivity	0.833	0.750	0.792	0.708	0.708	1.000	0.916
Area under curve	0.848	0.749	0.782	0.768	0.709	0.500	0.773

Accuracy, specificity, sensitivity, and area under the ROC curve are shown for each centrality measure. Ictogenic Centrality generally outperforms all other measures

Table 3 Performance metrics in a scale-free network

	Ictogenic Centrality	Latent Ictogenic Centrality	Outgoing PageRank	Incoming PageRank	Control Centrality	Out-degree	In-degree
Accuracy	0.944	0.940	0.944	0.796	0.776	0.436	0.788
Specificity	0.936	0.936	0.936	0.744	0.830	0.000	0.702
Sensitivity	0.954	0.945	0.954	0.862	0.706	1.000	0.899
Area under curve	0.977	0.976	0.976	0.860	0.830	0.500	0.858

Accuracy, specificity, sensitivity, and area under the ROC curve are shown for each centrality measure. IC, LIC, and outgoing PageRank each performed roughly the same

which accord with clinical data. In seeking to explain *why* particular brain regions were "influential seizers" from a graph-theoretic perspective, we identified two essential characteristics: (1) a node's in-degree (which determines the influence of that node on its neighbors), and (2) the non-neighboring in-degrees of a node's neighbors (which determines how susceptible such neighbors are to the influence of an ictogenic node). Combining these two features into a novel measure, Ictogenic Centrality (IC, defined in Eq. 3.3), we were able to use connectivity structure alone to accurately identify influential seizers from dynamical simulations (Figs. 4, 5). This measure is simple, has only one free parameter, and can be efficiently computed for large networks.

IC also accurately identified influential seizers in generic network topologies. It outperformed all comparison measures in a random network (Fig. 7), and it also outperformed all comparison measures, except for outgoing PageRank (which it tied), in a scale-free network (Fig. 8). The fact that outgoing PageRank can sometimes rival IC in identifying influential seizers should not be surprising, since outgoing PageRank takes a similar approach to IC: it assigns greater weight to outgoing connections that terminate on nodes with small in-degree. This helps validate the fundamental premises that underpin IC.

It should be noted, however, that IC is heuristically derived from the dynamics of the Epileptor model. IC should therefore be successful in clinical applications to the extent that the Epileptor model is correct in predicting that healthy brain regions exert a protective effect on ictogenic regions (Proix et al. 2014). Furthermore, discarding dynamical information inevitably leads to some degradation in the identification of influential nodes. This is seen most clearly with Brodmann area 6 in the frontal lobe, which in simulations enlisted a large number of nodes in each seizure event (Fig. 1), yet was not identified as influential by IC (Fig. 5a). Further investigation suggested that this node's influence was due to an exceptionally long seizure duration resulting from its very small in-degree (a finding consistent with previous work by Proix et al. (2014)). It was possible to devise other centrality measures which modeled the dependence of seizure duration on in-degree in order to successfully identify Brodmann area 6 as influential, but such measures were overly contrived, required several additional parameters, and failed to improve accuracy above the level attained by IC. Overall, the highly accurate identification of influential seizers exhibited by IC suggests that ictogenic in-degree and non-neighboring in-degree are essential features in a network Epileptor model of focal epilepsy.

The fact that our results rely on information about the *direction* of brain connections may help to explain some results in previous network epilepsy studies. For example, Hutchings et. al. used the model of Benjamin et al. (2012) to model seizure dynamics on diffusion MRI-derived connectomes of patients with TLE (Hutchings et al. 2015). They identified brain regions that seized frequently in their model and found that most were highly connected hubs; however, not all hubs were frequent seizers. They were also unable to identify any other network measures that correlated with critical nodes in their model. Our results suggest that this may have been due to using MRI-derived connectivity data, since the directionality of connections appears to be essential to understanding seizure spread. This work therefore motivates experimental comparison of seizure dynamics with *directed* connectivity data. This could feasibly be accomplished with rodents (Oh et al. 2014) or macaques (Chen et al. 2013).

Obtaining directed human connectomes is obviously more challenging, but fMRI-derived effective connectivity (Frässle et al. 2018) could perhaps be combined with diffusion MRI-derived structural connectivity.

Our results suggest several novel clinical approaches to controlling seizure propagation. Rather than resecting the entire seizure focus, for example, it may be possible to sever connections from the focus to brain regions with low non-neighboring in-degree (Fig. 6), effectively choking off the "escape routes" of the seizure. In many circumstances, of course, the necessary connections would be surgically inaccessible. In situations with a well-defined epileptogenic zone in eloquent neocortex, however, the multiple subpial transections (MST) approach is sometimes used to sever easily accessible lateral gray matter connections (Englot 2018). In such operations, targeting only connections to brain regions with low non-neighboring in-degree could potentially minimize the number of connections to be severed.

For cases of medication-resistant epilepsy in which surgical resection or MST is impossible, the nascent field of brain stimulation holds promise (Bergey et al. 2015; Klinger and Mittal 2016). Both deep brain stimulation (DBS) and responsive neurostimulation (RNS) have shown some initial success in decreasing seizure frequency in several clinical studies (Fisher et al. 2010; Velasco et al. 2006; Morrell 2011; Bergey et al. 2015), although at this point neurostimulation rarely leads to seizure freedom (Englot et al. 2017). Our results from Fig. 2 suggest that increased input to the seizure focus from healthy brain regions may prevent seizure spread. Current antiepileptic stimulation protocols might therefore be improved by using the LFP from a region outside the seizure propagation zone as a control signal to the seizure focus, effectively increasing the ictogenic in-degree. (It would of course be extremely important to ensure that the seizure *never* spread to this control brain region—or if it did that some mechanism was in place to terminate the control signal.) Novel approaches such as these should initially be explored in animal models whose directed meso-scale connectomes have been mapped. The kainic acid model of focal epilepsy would be a sensible starting point, since it has already been used to study DBS in macaques (Chen et al. 2014) and rodents (Chen et al. 2017).

Our results suggest that brain regions in the temporal and frontal lobes may be more susceptible to spreading focal seizures (Cossu et al. 2005) due to their baseline connectivity, since they tend to feature smaller in-degree and to project more numerous connections to other nodes with small non-neighboring in-degree. Some cases of focal epilepsy may therefore result not from pathological network reorganization, but rather from insult to a brain region that is already well-situated to hijack its neighbors. Future experimental and clinical investigation is necessary in order to explore this hypothesis.

5 Supplementary Information

5.1 The Influence of In-Degree on Ictogenicity and Seizure Duration

The influence of in-degree on seizure spread, shown in Fig. 2 for node MT, was observed in many other high out-degree nodes. Figure 9 shows three other nodes that

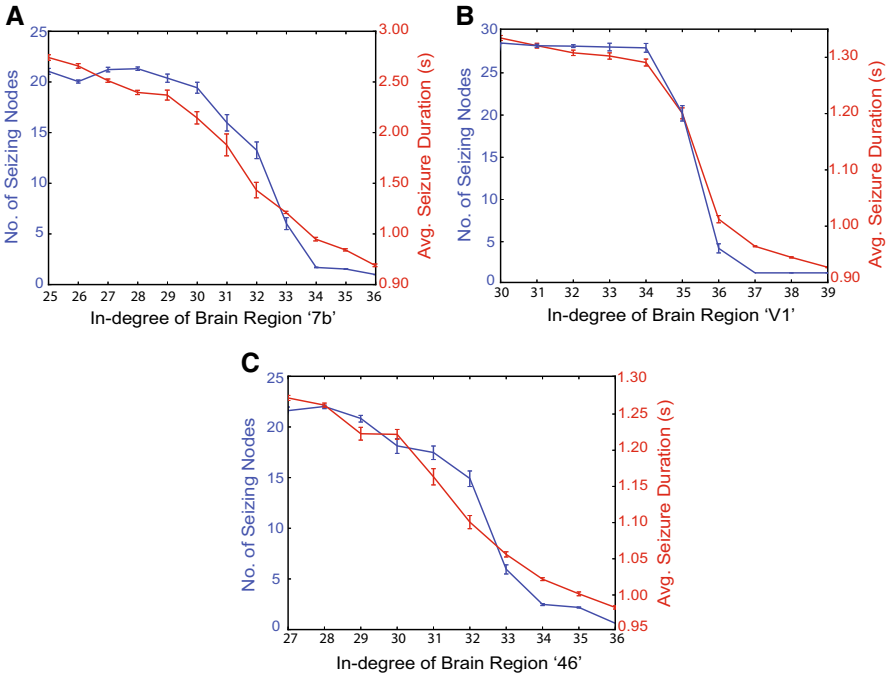

Fig. 9 High out-degree nodes become influential when incoming connections are severed. Brain regions 7b (out-degree: 62), V1 (out-degree: 38), and 46 (out-degree: 44) were not influential under baseline macaque connectivity. However, as incoming connections were progressively deleted, they became capable of spreading seizures throughout the network. Blue lines depict average number of nodes spread to, while red lines show average seizure duration. Error bars represent standard error of the mean over fifty simulations, each of which involved removal of a different set of randomly selected incoming connections (Color figure online)

became influential after a few incoming connections were deleted. As with node MT, the transition to seizure spread correlated with increasing seizure duration.

5.2 Protective Effect of Neighboring Versus Non-neighboring Connections

To investigate the relative protective effect of neighboring versus non-neighboring connections on seizure spread, we analyzed the toy network depicted in Fig. 10a. The ictogenic node had two neighbors, labeled nodes 1 and 2, with node 1 receiving a connection (Connection 1) from a non-neighboring node and also sending a connection to node 2 (Connection 2). We investigated how seizure spread depended on the relative strengths of these two connections. The strength of Connection 1 served as a proxy for the *non-neighboring* in-degree of node 1, and the strength of Connection 2 served as a proxy for the *neighboring* in-degree of node 2. In these simulations, Connection 1 strengths of more than 5 directly prevented seizure spread to node 1.

Figure 10b shows that the protective effect of Connection 2 depended on the strength of Connection 1. When the strength of Connection 1 was < 7, Connection 2 was incapable of preventing seizure spread to node 2 (Fig. 10c). For Connection 1 strengths

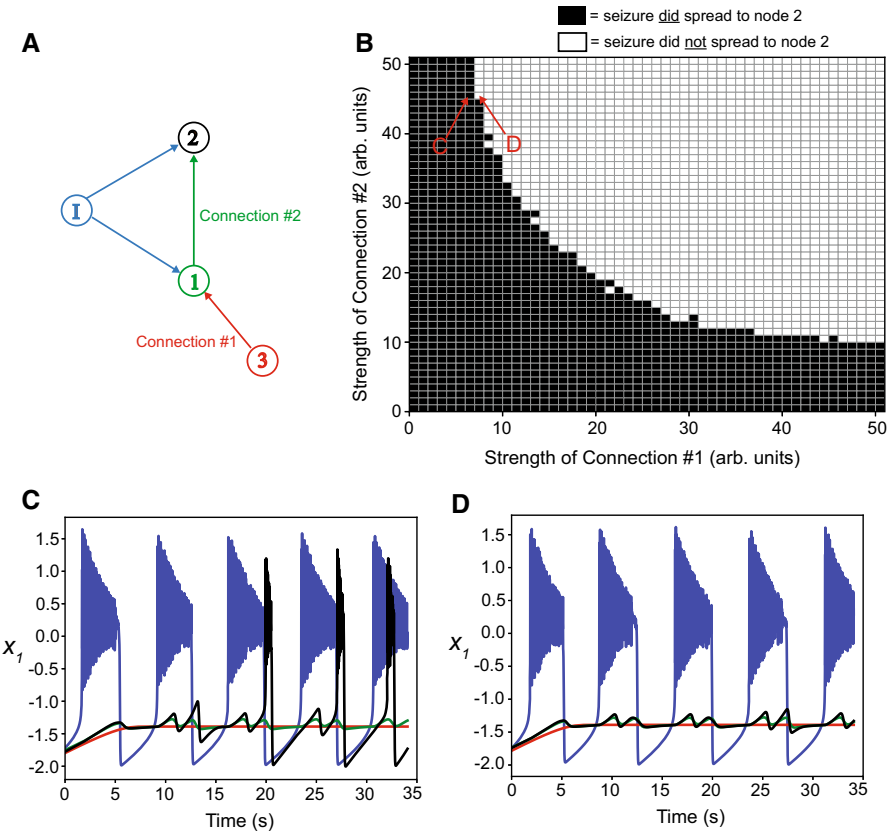

Fig. 10 Effect of neighboring versus non-neighboring connections in seizure spread. **a** Toy network used to explore how the protective effect of neighboring connections (represented by Connection 2) depends on the strength of non-neighboring connections (represented by Connection 1). **b** Summary of simulated parameter sweeps over the strengths of Connections 1 and 2. The ability of Connection 2 to prevent seizure spread to node 2 depended on the strength of Connection 1. **c** Example x_1 traces for a parameter combination (Connection 1 strength = 6, Connection 2 strength = 45) in which the seizure spread to node 2. x_1 is essentially the simulated voltage, but with noise removed for clarity. Color code is the same as in (**a**). **d** Example x_1 traces for a parameter combination in which the seizure did *not* spread to node 2. In this case, Connection 1 had a strength of 7, and Connection 2 had a strength of 45 (Color figure online)

$\geqslant 7$, Connection 2 was capable of exerting a protective effect on node 2 (Fig. 10d). Note, however, that the protective effect of this neighboring connection was initially much less than the protective effect of the non-neighboring connection: while a Connection 1 strength of 7 prevented seizure spread to node 1, Connection 2 required a strength of 45 to prevent seizure spread to node 2. As Connection 1's strength increased beyond 7, the strength required for Connection 2 to prevent seizure spread to node 2 diminished, but leveled off at $\approx$ 10. Therefore, neighboring connections are not as effective in protecting against seizure spread as non-neighboring connections.

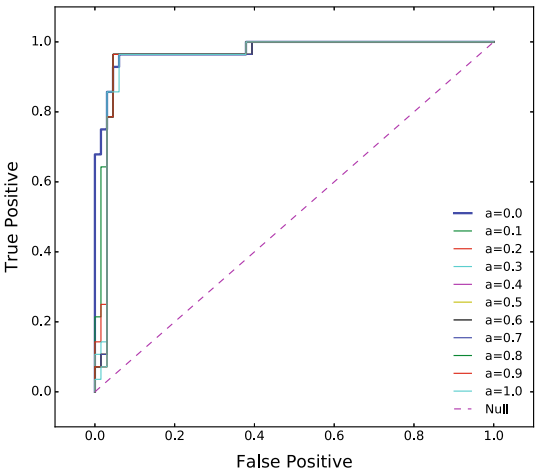

Fig. 11 Effects of neighboring in-degree weight on IC performance. ROC curves are displayed for values of a, which weights the neighboring in-degree term in the definition of Latent Ictogenic Centrality. All values of a give similar performance, with $a = 0$ giving slightly larger area under the curve than other values

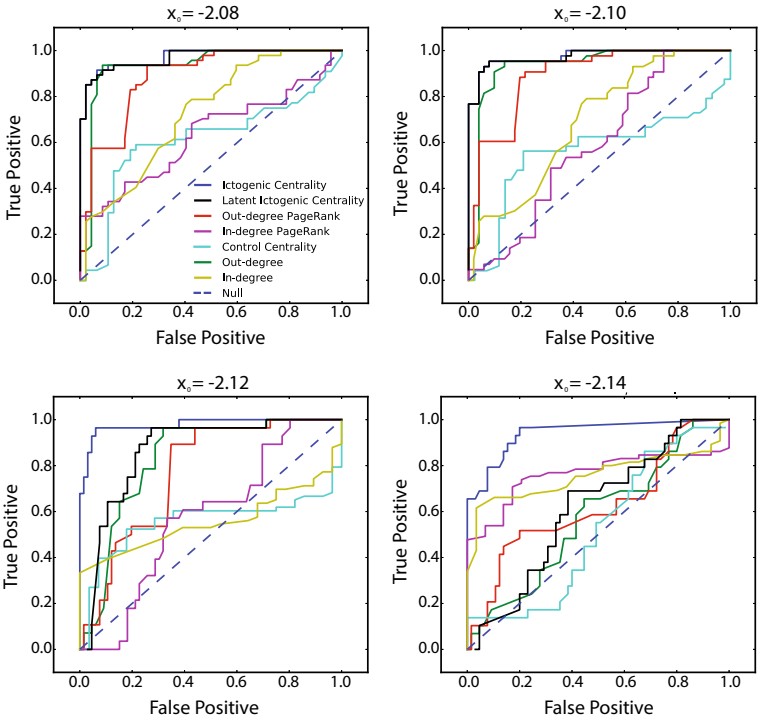

Fig. 12 Ictogenic Centrality performance comparison for different values of x_0. Each panel shows ROC curves of various centrality measures for a different value of the Epileptor parameter x_0. Ictogenic Centrality and Latent Ictogenic Centrality outperformed all other measures for all values of x_0, with Ictogenic Centrality's advantage increasing for more negative values of x_0

5.3 Effect of Neighboring In-Degree Term on IC Performance

Figure 11 displays the performance of Ictogenic Centrality in identifying influential nodes for various values of a in Eq. 3.1. All values give relatively similar areas under the ROC curve, although $a = 0$ slightly outperforms the rest.

5.4 Performance of Ictogenic Centrality for Various Values of x_0

The Epileptor parameter x_0 determines how susceptible a node is to seizing. Isolated nodes with $x_0 > -2.05$ seize intrinsically, while those with $x_0 < -2.05$ require ictogenic input to seize. In any one simulation, we followed previous work (Jirsa et al. 2014) by identifying one ictogenic node and inducing it to seize by setting $x_0 = -1.60$. In our main study, we set x_0 for all other nodes to -2.12. Figure 12 depicts results for three other non-ictogenic values of x_0. As in the main study, for each value of x_0, we conducted a sweep over coupling strength and selected the smallest value for which seizures spread appreciably throughout the network. For values more negative than -2.14 (far from the ictogenic threshold), seizures did not spread throughout the network for any coupling strength. As the figure shows, Ictogenic Centrality tended to outperform all other measures for all values of x_0, although it was rivaled by Latent Ictogenic Centrality and out-degree for x_0 values approaching the ictogenic threshold.

Acknowledgements Special thanks to Bill Stacey and Steve Gliske for their helpful comments on this paper.

Funding This work was supported by National Institutes of Health [R01-NS094399], the National Science Foundation [1560061], and the Ohio Wesleyan Summer Science Research Program.

References

Bakker, R., Wachtler, T., Diesmann, M.: Cocomac 2.0 and the future of tract-tracing databases. Front. Neuroinform. **6**, 30 (2012)

Barabási, A.-L., Albert, R.: Emergence of scaling in random networks. Science **286**(5439), 509–512 (1999)

Bartolomei, F., Lagarde, S., Wendling, F., McGonigal, A., Jirsa, V., Guye, M., Bénar, C.: Defining epileptogenic networks: contribution of seeg and signal analysis. Epilepsia **58**(7), 1131–1147 (2017)

Benjamin, O., Fitzgerald, T.H.B., Ashwin, P., Tsaneva-Atanasova, K., Chowdhury, F., Richardson, M.P., Terry, J.R.: A phenomenological model of seizure initiation suggests network structure may explain seizure frequency in idiopathic generalised epilepsy. J. Math. Neurosci. **2**(1), 1 (2012)

Bergey, G.K., Morrell, M.J., Mizrahi, E.M., Goldman, A., King-Stephens, D., Nair, D., Srinivasan, S., Jobst, B., Gross, R.E., Shields, D.C., et al.: Long-term treatment with responsive brain stimulation in adults with refractory partial seizures. Neurology **84**(8), 810–817 (2015)

Bernhardt, B.C., Bonilha, L., Gross, D.W.: Network analysis for a network disorder: the emerging role of graph theory in the study of epilepsy. Epilepsy Behav. **50**, 162–170 (2015)

Bonilha, L., Nesland, T., Martz, G.U., Joseph, J.E., Spampinato, M.V., Edwards, J.C., Tabesh, A.: Medial temporal lobe epilepsy is associated with neuronal fibre loss and paradoxical increase in structural connectivity of limbic structures. J. Neurol. Neurosurg. Psychiatry **89**(9), 903–909 (2012)

Bonilha, L., Jensen, J.H., Baker, N., Breedlove, J., Nesland, T., Lin, J.J., Drane, D.L., Saindane, A.M., Binder, J.R., Kuzniecky, R.I.: The brain connectome as a personalized biomarker of seizure outcomes after temporal lobectomy. Neurology **84**(18), 1846–1853 (2015)

Breakspear, M., Roberts, J.A., Terry, J.R., Rodrigues, S., Mahant, N., Robinson, P.A.: A unifying explanation of primary generalized seizures through nonlinear brain modeling and bifurcation analysis. Cerebral Cortex **16**(9), 1296–1313 (2005)

Buckmaster, P.S., Zhang, G.F., Yamawaki, R.: Axon sprouting in a model of temporal lobe epilepsy creates a predominantly excitatory feedback circuit. J. Neurosci. **22**(15), 6650–6658 (2002)

Chen, N., Liu, C., Yan, N., Wei, H., Zhang, J., Ge, Y., Meng, F.: A macaque model of mesial temporal lobe epilepsy induced by unilateral intrahippocampal injection of kainic acid. PLoS ONE **8**(8), e72336 (2013)

Chen, N., Gao, Y., Yan, N., Liu, C., Zhang, J.-G., Xing, W.-M., Kong, D.-M., Meng, F.-G.: High-frequency stimulation of the hippocampus protects against seizure activity and hippocampal neuronal apoptosis induced by kainic acid administration in macaques. Neuroscience **256**, 370–378 (2014)

Chen, Y.-C., Zhu, G.-Y., Wang, X., Shi, L., Jiang, Y., Zhang, X., Zhang, J.-G.: Deep brain stimulation of the anterior nucleus of the thalamus reverses the gene expression of cytokines and their receptors as well as neuronal degeneration in epileptic rats. Brain Res. **1657**, 304–311 (2017)

Cossu, M., Cardinale, F., Castana, L., Citterio, A., Francione, S., Tassi, L., Benabid, A.L., Lo Russo, G.: Stereoelectroencephalography in the presurgical evaluation of focal epilepsy: a retrospective analysis of 215 procedures. Neurosurgery **57**(4), 706–718 (2005)

Crossley, N.A., Mechelli, A., Scott, J., Carletti, F., Fox, P.T., McGuire, P., Bullmore, E.T.: The hubs of the human connectome are generally implicated in the anatomy of brain disorders. Brain **137**(8), 2382–2395 (2014)

Crunelli, V., Leresche, N.: Childhood absence epilepsy: genes, channels, neurons and networks. Nat. Rev. Neurosci. **3**(5), 371 (2002)

Da Silva, F.L., Blanes, W., Kalitzin, S.N., Parra, J., Suffczynski, P., Velis, D.N.: Epilepsies as dynamical diseases of brain systems: basic models of the transition between normal and epileptic activity. Epilepsia **44**(12), 72–83 (2003)

de Solla Price, D.: A general theory of bibliometric and other cumulative advantage processes. J. Am. Soc. Inf. Sci. **27**(5), 292–306 (1976)

Deco, G., Jirsa, V.K., McIntosh, A.R., Sporns, O., Kotter, R.: Key role of coupling, delay, and noise in resting brain fluctuations. Proc. Natl. Acad. Sci. USA **106**, 10302–10307 (2009)

Elsharkawy, A.E., Behne, F., Oppel, F., Pannek, H., Schulz, R., Hoppe, M., Pahs, G., Gyimesi, C., Nayel, M., Issa, A., et al.: Long-term outcome of extratemporal epilepsy surgery among 154 adult patients. J. Neurosurg. **108**(4), 676–686 (2008)

Engel Jr., J., Wiebe, S., French, J., Sperling, M., Williamson, P., Spencer, D., Gumnit, R., Zahn, C., Westbrook, E., Enos, B.: Practice parameter: temporal lobe and localized neocortical resections for epilepsy. Epilepsia **44**(6), 741–751 (2003)

Englot, D.J.: A modern epilepsy surgery treatment algorithm: Incorporating traditional and emerging technologies. Epilepsy Behav. **80**, 68–74 (2018)

Englot, D.J., Birk, H., Chang, E.F.: Seizure outcomes in nonresective epilepsy surgery: an update. Neurosurg. Rev. **40**, 181–194 (2017)

Fisher, R., Salanova, V., Witt, T., Worth, R., Henry, T., Gross, R., Oommen, K., Osorio, I., Nazzaro, J., Labar, D., et al.: Electrical stimulation of the anterior nucleus of thalamus for treatment of refractory epilepsy. Epilepsia **51**(5), 899–908 (2010)

Frässle, S., Lomakina, E.I., Kasper, L., Manjaly, Z.M., Leff, A., Pruessmann, K.P., Buhmann, J.M., Stephan, K.E.: A generative model of whole-brain effective connectivity. NeuroImage **179**, 505–529 (2018)

Ghosh, A., Rho, Y., McIntosh, A.R., Kötter, R., Jirsa, V.K.: Noise during rest enables the exploration of the brain's dynamic repertoire. PLoS Computat. Biol. **4**(10), e1000196 (2008)

Goodfellow, M., Rummel, C., Abela, E., Richardson, M.P., Schindler, K., Terry, J.R.: Estimation of brain network ictogenicity predicts outcome from epilepsy surgery. Sci. Rep. **6**, 29215 (2016)

Goulas, A., Bastiani, M., Bezgin, G., Uylings, H.B.M., Roebroeck, A., Stiers, P.: Comparative analysis of the macroscale structural connectivity in the macaque and human brain. PLoS Comput. Biol. **10**(3), e1003529 (2014)

Hindmarsh, J., Cornelius, P.: The development of the Hindmarsh–Rose model for bursting. In: Coombes, S., Bressloff, P.C. (eds.) Bursting: The Genesis of Rhythm in the Nervous System, pp. 3–18. World Scientific (2005)

Hindmarsh, J.L., Rose, R.M.: A model of neuronal bursting using three coupled first order differential equations. Proc. R. Soc. Lond. B **221**(1222), 87–102 (1984)

Hutchings, F., Han, C.E., Keller, S.S., Weber, B., Taylor, P.N., Kaiser, M.: Predicting surgery targets in temporal lobe epilepsy through structural connectome based simulations. PLoS Comput. Biol. **11**(12), e1004642 (2015)

Hwang, D.-U., Chavez, M., Amann, A., Boccaletti, S.: Synchronization in complex networks with age ordering. Phys. Rev. Lett. **94**(13), 138701 (2005)

Ji, G.-J., Zhang, Z., Qiang, X., Zang, Y.-F., Liao, W., Guangming, L.: Generalized tonic-clonic seizures: aberrant interhemispheric functional and anatomical connectivity. Radiology **271**(3), 839–847 (2014)

Jirsa, V.K., Stacey, W.C., Quilichini, P.P., Ivanov, A.I., Bernard, C.: On the nature of seizure dynamics. Brain **137**(8), 2210–2230 (2014)

Jirsa, V.K., Proix, T., Perdikis, D., Woodman, M.M., Wang, H., Gonzalez-Martinez, J., Bernard, C., Bénar, C., Guye, M., Chauvel, P., et al.: The virtual epileptic patient: individualized whole-brain models of epilepsy spread. Neuroimage **145**, 377–388 (2017)

Kaiser, M., Hilgetag, C.C.: Nonoptimal component placement, but short processing paths, due to long-distance projections in neural systems. PLoS Comput. Biol. **2**(7), e95 (2006)

Kale, P., Zalesky, A., Gollo, L.L.: Estimating the impact of structural directionality: how reliable are undirected connectomes? Netw. Neurosci. **2**(2), 1–51 (2018)

Kalitzin, S.N., Velis, D.N., da Silva, F.H.L.: Stimulation-based anticipation and control of state transitions in the epileptic brain. Epilepsy Behav. **17**(3), 310–323 (2010)

Khambhati, A.N., Davis, K.A., Lucas, T.H., Litt, B., Bassett, D.S.: Virtual cortical resection reveals push-pull network control preceding seizure evolution. Neuron **91**(5), 1170–1182 (2016)

Kim, J.B., Suh, S., Seo, W.-K., Oh, K., Koh, S.-B., Kim, J.H.: Altered thalamocortical functional connectivity in idiopathic generalized epilepsy. Epilepsia **55**(4), 592–600 (2014)

Klinger, N.V., Mittal, S.: Clinical efficacy of deep brain stimulation for the treatment of medically refractory epilepsy. Clin. Neurol. Neurosurg. **140**, 11–25 (2016)

Kötter, R.: Online retrieval, processing, and visualization of primate connectivity data from the cocomac database. Neuroinformatics **2**(2), 127–144 (2004)

Kötter, R., Wanke, E.: Mapping brains without coordinates. Philos. Trans. R. Soc. B: Biol. Sci. **360**(1456), 751–766 (2005)

Kwan, P., Sander, J.W.: The natural history of epilepsy: an epidemiological view. J. Neurol. Neurosurg. Psychiatry **75**(10), 1376–1381 (2004)

Liao, W., Zhang, Z., Pan, Z., Mantini, D., Ding, J., Duan, X., Luo, C., Guangming, L., Chen, H.: Altered functional connectivity and small-world in mesial temporal lobe epilepsy. PLoS ONE **5**(1), e8525 (2010)

Lytton, W.W.: Computer modelling of epilepsy. Nat. Rev. Neurosci. **9**(8), 626 (2008)

Manford, M., Hart, Y.M., Sander, J.W.A.S., Shorvon, S.D.: The national general practice study of epilepsy: the syndromic classification of the international league against epilepsy applied to epilepsy in a general population. Arch. Neurol. **49**(8), 801–808 (1992)

Maynard, L.M., Leach, J.L., Horn, P.S., Spaeth, C.G., Mangano, F.T., Holland, K.D., Miles, L., Faist, R., Greiner, H.M.: Epilepsy prevalence and severity predictors in MRI-identified focal cortical dysplasia. Epilepsy Res. **132**, 41–49 (2017)

Morgan, R.J., Soltesz, I.: Nonrandom connectivity of the epileptic dentate gyrus predicts a major role for neuronal hubs in seizures. Proc. Natl. Acad. Sci. **105**(16), 6179–6184 (2008)

Mormann, F., Andrzejak, R.G., Elger, C.E., Lehnertz, K.: Seizure prediction: the long and winding road. Brain **130**(2), 314–333 (2006)

Morrell, M.J.: Responsive cortical stimulation for the treatment of medically intractable partial epilepsy. Neurology **77**(13), 1295–1304 (2011)

Newman, M.: Networks. Oxford University Press, Oxford (2018)

Oh, S.W., Harris, J.A., Ng, L., Winslow, B., Cain, N., Mihalas, S., Wang, Q., Lau, C., Kuan, L., Henry, A.M., et al.: A mesoscale connectome of the mouse brain. Nature **508**(7495), 207 (2014)

Page, L., Brin, S., Motwani, R., Winograd, T.: The pagerank citation ranking: bringing order to the web. Technical report, Stanford InfoLab (1999)

Pecora, L.M., Carroll, T.L.: Master stability functions for synchronized coupled systems. Phys. Rev. Lett. **80**(10), 2109 (1998)

Petkov, G., Goodfellow, M., Richardson, M.P., Terry, J.R.: A critical role for network structure in seizure onset: a computational modeling approach. Front. Neurol. **5**, 261 (2014)

Prayson, R.A., Estes, M.L.: Cortical dysplasia: a histopathologic study of 52 cases of partial lobectomy in patients with epilepsy. Hum. Pathol. **26**(5), 493–500 (1995)

Proix, T., Bartolomei, F., Chauvel, P., Bernard, C., Jirsa, V.K.: Permittivity coupling across brain regions determines seizure recruitment in partial epilepsy. J. Neurosci. **34**(45), 15009–15021 (2014)
Proix, T., Bartolomei, F., Guye, M., Jirsa, V.K.: Individual brain structure and modelling predict seizure propagation. Brain **140**(3), 641–654 (2017)
Semah, F., Broglin, D., Arzimanoglou, A., Cavalcanti, D., Baulac, M.: Is the underlying cause of epilepsy a major prognostic factor for recurrence? Neurology **51**, 1256–1262 (1998)
Shah, P., Bernabei, J., Kini, L., Ashourvan, A., Boccanfuso, J., Archer, R., Oechsel, K., Lucas, T.H., Bassett, D.S., Davis, K., et al.: High interictal connectivity within the resection zone is associated with favorable post-surgical outcomes in focal epilepsy patients. bioRxiv, pp. 459008 (2018)
Sinha, N., Dauwels, J., Kaiser, M., Cash, S.S., Brandon Westover, M., Wang, Y., Taylor, P.N.: Predicting neurosurgical outcomes in focal epilepsy patients using computational modelling. Brain **140**(2), 319–332 (2016)
Sørensen, A.T., Kokaia, M.: Novel approaches to epilepsy treatment. Epilepsia **54**(1), 1–10 (2013)
Spencer, S.S.: Neural networks in human epilepsy: evidence of and implications for treatment. Epilepsia **43**(3), 219–227 (2002)
Sveinbjornsdottir, S., Duncan, J.S.: Parietal and occipital lobe epilepsy: a review. Epilepsia **34**(3), 493–521 (1993)
Taylor, P.N., Baier, G.: A spatially extended model for macroscopic spike-wave discharges. J. Comput. Neurosci. **31**(3), 679–684 (2011)
Taylor, P.N., Goodfellow, M., Wang, Y., Baier, G.: Towards a large-scale model of patient-specific epileptic spike-wave discharges. Biol. Cybern. **107**(1), 83–94 (2013)
Terry, J.R., Benjamin, O., Richardson, M.P.: Seizure generation: the role of nodes and networks. Epilepsia **53**(9), e166–e169 (2012)
Vaessen, M.J., Jansen, J.F.A., Braakman, H.M.H., Hofman, P.A.M., De Louw, A., Aldenkamp, A.P., Backes, W.H.: Functional and structural network impairment in childhood frontal lobe epilepsy. PLoS ONE **9**(3), e90068 (2014)
van Diessen, E., Zweiphenning, W.J.E.M., Jansen, F.E., Stam, C.J., Braun, K.P.J., Otte, W.M.: Brain network organization in focal epilepsy: a systematic review and meta-analysis. PLoS ONE **9**(12), e114606 (2014)
Velasco, A.L., Velasco, F., Jiménez, F., Velasco, M., Castro, G., Carrillo-Ruiz, J.D., Fanghänel, G., Boleaga, B.: Neuromodulation of the centromedian thalamic nuclei in the treatment of generalized seizures and the improvement of the quality of life in patients with lennox–gastaut syndrome. Epilepsia **47**(7), 1203–1212 (2006)
Watts, D.J., Strogatz, S.H.: Collective dynamics of small-world networks. Nature **393**(6684), 440 (1998)
Wendling, F., Bartolomei, F., Bellanger, J.J., Chauvel, P.: Epileptic fast activity can be explained by a model of impaired gabaergic dendritic inhibition. Eur. J. Neurosci. **15**(9), 1499–1508 (2002)
Wendling, F., Chauvel, P., Biraben, A., Bartolomei, F.: From intracerebral eeg signals to brain connectivity: identification of epileptogenic networks in partial epilepsy. Front. Syst. Neurosci. **4**, 154 (2010)
World Health Organization: Neurological disorders: public health challenges. http://www.who.int/mental_health/neurology/neurological_disorders_report_web.pdf, p. 189 (2006). Accessed 11 Apr 2019

Affiliations

Joseph Emerson[1] · Amber Afelin[2] · Viesulas Sliupas[3] · Christian G. Fink[4]

✉ Christian G. Fink
finkt@gonzaga.edu

Joseph Emerson
jhemerso@owu.edu

Amber Afelin
aafelin@wesleyan.edu

Viesulas Sliupas
vsliupas@gmail.com

1 Ohio Wesleyan University, 61 South Sandusky Street, Delaware, OH 43015, USA

2 Wesleyan University, 45 Wyllys Avenue, Middletown, CT 06459, USA

3 Vacaville, USA

4 Gonzaga University, 502 East Boone Avenue, Spokane, WA 99258, USA